A potential function for neuronal exosomes: sequestering intracerebral amyloid-ß peptide

Authors: Kohei Yuyama[1]*, Hui Sun[1], Seigo Usuki[1], Shota Sakai[1], Hisatoshi Hanamatsu[1], Tetsuo Mioka[1, 2], Nobuyuki Kimura[3], Megumi Okada[4], Hidetoshi Tahara[4], Jun-ichi Furukawa[5], Naoki Fujitani[5], Yasuro Shinohara[5], and Yasuyuki Igarashi[1]

Affiliations:

(1) Laboratory of Biomembrane and Biofunctional Chemistry, Graduate School of Advanced Life Science, and Frontier Research Center for Post-Genome Science and Technology, Hokkaido University, Sapporo, Japan.

(2) Division of Molecular Interaction, Institute for Genetic Medicine, Graduate School of Life Science, Hokkaido University, Sapporo, Japan.

(3) Section of Cell Biology and Pathology, Department of Alzheimer's Disease Research, Center for Development of Advanced Medicine for Dementia, National Center for Geriatrics and Gerontology, Obu, Japan

(4) Department of Cellular and Molecular Biology, Graduate School of Biomedical Science, Hiroshima University, Hiroshima, Japan

(5) Laboratory of Medical and Functional Glycomics, Graduate School of Advanced Life Science, and Frontier Research Center for Post-Genome Science and Technology, Hokkaido University, Sapporo, Japan.

***Corresponding author:** Kohei Yuyama

Tel: +81(11)-706-9047

E-mail: kyuyama@pharm.hokudai.ac.jp

Abstract

Elevated amyloid-ß peptide (Aß) in brain contributes to Alzheimer's disease (AD) pathogenesis. We demonstrated the presence of exosome-associated Aß in the CSF of cynomolgus monkeys and APP transgenic mice, which notably decreased in aging animals. We also determined that neuronal exosomes, but not glial exosomes, had abundant GSLs and could capture Aß. Infusion of neuronal exosomes into brains of APP transgenic mice decreased Aß and amyloid depositions, similar to previous reports of neuroblastoma-derived exosomes. These findings highlight the role of neuronal exosomes in Aß clearance, and suggest their downregulation might relate to Aß accumulation, which serves to develop AD pathology.

Keywords

Exosome, Amyloid-ß peptide, Alzheimer's disease, Cynomolgus monkey, APP transgenic mouse, Cerebrospinal fluid

Abbreviations

Aß, amyloid-ß peptide; AD, Alzheimer disease; APP, amyloid-ß precursor protein; GSL, glycosphingolipid; CSF, cerebrospinal fluid; N2a, Neuro2a; EGCase, endoglycoceramidase

Introduction

A pathological feature of Alzheimer's disease (AD) is the presence of senile plaques, extracellular amyloid depositions of amyloid-ß peptide (Aß). Aß is generated by the processing of amyloid precursor protein (APP), and is maintained at a steady state in normal brain. However, disruption of the balance in Aß metabolism contributes to the formation of toxic Aß assemblies and amyloid depositions, which are linked to AD pathogenesis. Recently, exosomes, a subtype of secreted vesicles, were reported to associate with extracellular Aß in cultures of APP-expressing neuroblastoma cells [1, 2]. Similarly, our previous study both in vitro and in vivo demonstrated that exosomes released from neuroblastoma N2a can bind Aß on their surface glycosphingolipids (GSLs) and these Aß-bound exosomes are then internalized by microglia for degradation [3, 4]. This suggests that N2a-derived exosomes may act for Aß elimination in brain. However, it remains unclear whether the exosomes, which originate from cells resident in the central nervous system, also contribute to Aß metabolism.

Materials and Methods

Animals.

Wild type C57BL/6 mice and mice expressing the human APP bearing the Swedish and Indiana (KM670/671NL, V717F) mutations (J20) were obtained from SLC Inc. (Hamamatsu, Japan) and the Jackson Laboratory (Bar Harbor, ME), respectively. All animal procedures were approved by the Animal Care Committees of Hokkaido University.

Monkey and murine samples

Cynomolgus monkeys (Macaca fascicularis) were housed at the Tsukuba Primate Research Center (TPRC), National Institute of Biomedical Innovation (NIBIO), Ibaraki, Japan. Monkey CSF samples were obtained by lumbar puncture. Nine CSF samples were from young monkeys (4-8 years old), 8 from adult monkeys (11-21 years old), and 4 from aged monkeys (24-36 years old). Each CSF sample was used for exosome isolation without prior freezing. The parietal lobes of 20 monkeys were used for Western blotting and ELISA. All animals were bred and maintained in an air-conditioned room at the TPRC with controlled illumination (12 h light/12 h dark), temperature (25 ± 2ºC), humidity (60 ± 5%), and ventilation (10 cycles/h), and were

given 70 g of commercial food and 100 g of apples daily, with unlimited access to tap water [5]. The maintenance of animals was conducted according to rules of the TPRC at NIBIO regarding the care, use, and biohazard countermeasures of laboratory animals. All animal experiments were conducted according to the guidelines of the Animal Care and Use Committee of the NIBIO, Japan.

Mouse CSF was sampled from the cisterna magna following protocols previously reported [6]. Each 50 µL of CSF was collected from 2-month-old C57BL/6 mice or APP mice at the indicated ages.

Cell cultures.

Primary neuron cultures were prepared from the cerebral cortices of mouse brains on embryonic day 15 as described previously [3]. Primary glial cultures were prepared from the mouse cortex according to published methods with minor modifications [7, 8]. Briefly, the neocortex was removed from each 2-day-old mouse pup, dissociated in a dissociation solution (Sumitomo Bakelite, Tokyo, Japan), and plated in DMEM and 10% fetal bovine serum (FBS). After being cultured for 14 days, the microglia were detached by shaking, and the separate cells were cultured in DMEM/5% FBS. The astrocytes remaining in the flasks were cultured in DMEM/10% FBS. The resultant glial cells were cultured for two days and used for further analysis.

Exosome isolation.

Exosomes were prepared from supernatants of primary cultures as described previously [3]. Briefly, after culture of cells for one day, the culture supernatants were sequentially centrifuged at 2,000g for 10 min, and at 10,000g for 30 min, and at 100,000g for 1 hour to obtain exosomes as pellets. Using this same method, exosomes were also isolated from the CSF samples of APP mice or monkeys.

Electron microscopy.

Exosomes were stained with phosphotungstic acid. For immunolabeling, the exosomes were incubated with anti-Aß antibody (4G8) then 10 nm gold-coupled anti-IgG. Images were taken with JEM-ARM200F (JEOL Ltd., Tokyo, Japan) transmission electron microscope.

Western Blotting.

To detect target proteins, we employed monoclonal antibodies against Alix, GM130, Transferrin receptor (BD Biosciences), and Aß (6E10, Signet, Dedham, MA), and a polyclonal antibody against flottilin-1(Santa Cruz Biotechnology). Ganglioside GM1, was detected by cholera toxin B subunit (Sigma).

Fluorescence labeling for the exosomes.

Labeling of the exosomes was performed using PKH26 (Sigma) as described previously [3].

Analysis of particle size and number.

The exosomes collected from primary cultures of neurons and CSF samples were suspended in PBS, and a qNano System (Izon Science, Ltd) employed to analyze the particle size and densities. CPC100 was used as the calibration sample.

Exosome administration into mouse brains.

The experiment was performed as previously described [4]. Briefly, mice were continuously treated with exosomes (2 mg protein/ml) or PBS by Alzet minipump at 0.25 µl/h for 14 days. The Brain Infusion Kit were implanted into the right hippocampus using a stereotactic instrument. One hemibrain was fixed for immunohistochemistry, and the other was frozen for use in ELISA.

Immunohistochemistry and thioflavin-S (ThS) staining

Immunostaining and ThS staining were performed as described previously [4].

Aß ELISA.

$Aß_{1-40}$ and $Aß_{1-42}$ levels were determined using an ELISA kit (Wako, Osaka, Japan) as previously described [4].

Measurement of Glycosphingolipids (GSLs).

Levels of GSLs in the exosomes of primary cultures were measured as described previously [4]. After their extraction, the GSLs were enzymatically digested with EGCase I and II, further purified by glycoblotting, then analyzed by MALDI-TOF MS.

Endoglycosylceramidase (EGCase)

Exosomes (1 mg protein/ml) were incubated with 0.5U/ml EGCase II (Takara Bio Inc., Shiga, Japan) at 37ºC for 15 h in PBS.

Thioflavin assay

Thioflavin-T (ThT) assay was performed as previously published [4].

Aß binding assay.

Fluorescent $Aß_{1-42}$ (25 µM) was incubated with the PKH26-labeled exosomes (treated with or without EGCase) in serum-free medium at 37ºC for 5 h. The exosomes and bound Aß were observed after wash out free Aß.

Results

Exosomes associate with Aß in the CSF of non-human primates.

The nonhuman primate cynomolgus monkey is widely used for AD-related preclinical studies [9]. In the monkey brains, Aß naturally increases in an age-dependent manner (Fig. 1A) as described in the previous reports [10, 11]. To investigate the effect of exosomes originating from brain cells against Aß metabolism, we isolated exosomes from monkey CSF, then measured the Aß levels in the exosome fractions. The CSF-derived exosomes were confirmed by electron microscopy to mainly consist of small membrane vesicles 50-200 nm in diameter (Fig. 1B), similar to previously described [12]. The exosome size was further verified by a nanoparticle analyzer, which found the sizes to range from 100 to 200 nm (Fig. 1C). The exosomal markers were also identified in the CSF-exosome fractions (Fig. 1D). We found that Aß was detectable in all CSF-derived exosome fractions but that the levels of exosome-associated Aß were markedly lower in the adult and aged brains compared to the young subjects (Fig. 1E). The level of free Aß, which was not associated with the exosomes in the CSF, declined only in the aged brains (Supplemental Fig. 1). These results suggest that the function of exosomes transporting Aß in the central nervous system may deteriorate with age (>11-year-old).

Age-related alterations in the number of exosomes in primary neuronal cultures and

APP transgenic mouse CSF.

Neuronal cell cultures are widely used as models to study the molecular mechanisms of aging. We collected the exosomes from primary cultures of cortical neurons at 1, 7, or 14 day in vitro (DIV) and found that there were significant reductions in the number of particles at DIV14 compared to those at DIV1 or DIV7 (Supplemental Fig. 2A). While exosomal GSLs, especially sialylated GSLs, kept rising up to DIV14 (Supplemental Fig. 2B). These suggest that a reduction in exosome release might occur during aging, with maintaining the capacity of individual exosome to bind with Aß.

To investigate whether the above findings in the non-human primates and in the neuronal cultures are also observed in APP transgenic mice, we collected the exosomes from CSF of 13-month-old APP mice and examined them for the presence of Aß, using western blot analysis and electron microscopy with immunolabeling (Fig. 2A, B). We then quantified the exosomes isolated from APP mouse CSF at ages 2 to 23 months. Compared to the number of CSF-exosomes isolated from young mice (2-3 months old), the densities of exosomes in mice aged 6-7 months decreased; these low levels were maintained through 12-13 months of age, thereafter drastically declined in 23-month-old mice (Fig. 2C). We also showed marked reduction in Aß levels in the CSF-exosomes between 2- and 23-month-old APP transgenic mice (2.19 ± 0.36 nM and 0.015 ± 0.012 nM, respectively), in accordance with those in the monkey CSF with age. In contrast, Aß levels in the brain tissues continued rising in mice from ages 6-7 months to 23 months. The above data raised the possibility that endogenous exosomes released from brain cells may play a role in modulating Aß metabolism.

GSL-enriched neuronal exosomes, but not glial exosomes, associate with Aß.

We previously determined that the enriched glycans of the GSLs are essential for Aß binding and assembly on N2a-exosomes [3]. To examine this in our current model, we collected exosomes from primary cultures of rodent cortical neurons, astrocytes and microglia, and determined the profiles of their GSL-derived glycans and their propensity for trapping Aß. We found that there were significantly more GSLs in neuronal exosomes than in exosomes from glial cells (Fig. 3A). Sialylated GSLs were also abundant in the neuronal exosomes; in particular, trisialoganglioside GT1 was found in only neuronal exosomes (Supplemental table. 1). Ganglioside GM1, which has been reported to bind Aß in AD brains, was also highly enriched in neuronal exosomes

(Supplemental Fig. 3 and table). Accordingly, neuronal exosomes, but not glial exosomes, associated with Aß (Fig. 3B). In ThT assays for amyloid fibril detection, fluorescence intensities were enhanced after a 5 h-incubation with Aß (Fig. 3C). Pretreatment of the neuronal exosomes with EGCase largely prevented the ThT fluorescence (Fig. 3C), indicating that the GSLs abundant in the neuronal exosomes contributed to the potency of the exosomes to bind Aß.

Administration of neuronal exosomes decreases Aß pathology in APP mouse brains.

To assess the effect of the exosomes derived from primary neurons on amyloid pathology, we continuously administered the exosomes into the right hippocampus of 13-month-old APP mice. We found that the exosomes induced marked reductions in Aß immunoreactive burdens (Fig. 4A, B) and ThS-positive plaques (Fig. 4C) in the treated hippocampus. Tissue levels of Aßs were also significantly decreased following the exosome infusion (Fig. 4D). These findings demonstrate that the treatment with neuronal exosomes effectively ameliorates Aß pathology in APP mice, suggesting a novel role for neuronal exosomes in clearing Aß in brain.

Discussion

Our study shown here demonstrated that exosomes are presented in monkey and murine CSF. The exosomes collected from monkey CSF at all ages contained Aß (Fig. 1E), demonstrating that endogenous exosomes are also coupled with Aß. In addition, the numbers of exosomes in the CSF of APP transgenic mice changed in an age dependent manner (Fig. 2C). It remains unclear which age-related factors would modulate exosome numbers, although the impairment of endocytic transport might be a potent possibility. Endocytic disturbances, such as endosome enlargement, are observed in aged monkey brains, with concomitant higher expression of Rab GTPases, which are responsible for the endosome transport [13, 14]. In addition, the dysfunction of dynein, a microtubule-associated protein active in endosome trafficking, has also been observed in aged monkey brains [13]. Notably, knockdown of dynein reduced exosome release from N2a cells [13]. Considering the appearance of endocytic pathology in early AD pathogenesis [15, 16], disturbance of intracellular transport might mediate the reduction of exosomes, eventually leading to Aß accumulation in the aged brains.

Our study reported here clearly demonstrated that intracerebral infusion of neuronal

exosomes results in decreases in Aß levels and amyloid deposition in the brains of APP transgenic mice (Fig. 4). It is noteworthy that another pathological agent of AD, tau, can be collected from the CSF-exosomes of early AD patients [17], raising the possibility that exosomes modulate multiple factors associated with AD pathogenesis. The improvement of endogenous exosome generation might serve as a novel approach for treating or preserving AD.

Acknowledgement

This work was supported by Creation of Innovation Centers for Advanced Interdisciplinary Research Areas Program, Ministry of Education, Culture, Sports, Science and Technology, Japan.

References

1. Rajendran, L., Honsho, M., Zahn, T. R., Keller, P., Geiger, K. D., Verkade, P. & Simons, K. (2006) Alzheimer's disease beta-amyloid peptides are released in association with exosomes, *Proc Natl Acad Sci USA.* **103**, 11172-7.

2. Vingtdeux, V., Hamdane, M., Loyens, A., Gele, P., Drobeck, H., Begard, S., Galas, M. C., Delacourte, A., Beauvillain, J. C., Buee, L. & Sergeant, N. (2007) Alkalizing drugs induce accumulation of amyloid precursor protein by-products in luminal vesicles of multivesicular bodies, *J Biol Chem.* **282**, 18197-205.

3. Yuyama, K., Sun, H., Mitsutake, S. & Igarashi, Y. (2012) Sphingolipid-modulated exosome secretion promotes clearance of amyloid-beta by microglia, *J Biol Chem.* **287**, 10977-89.

4. Yuyama, K., Sun, H., Sakai, S., Mitsutake, S., Okada, M., Tahara, H., Furukawa, J., Fujitani, N., Shinohara, Y. & Igarashi, Y. (2014) Decreased Amyloid-beta Pathologies by Intracerebral Loading of Glycosphingolipid-enriched Exosomes in Alzheimer Model Mice, *J Biol Chem.* **289**, 24488-98.

5. Tsuchida, J., Yoshida, T., Sankai, T. & Yasutomi, Y. (2008) Maternal behavior of laboratory-born, individually reared long-tailed macaques (Macaca fascicularis), *Journal of the American Association for Laboratory Animal Science : JAALAS.* **47**, 29-34.

6. DeMattos, R. B., Bales, K. R., Parsadanian, M., O'Dell, M. A., Foss, E. M., Paul, S. M. & Holtzman, D. M. (2002) Plaque-associated disruption of CSF and plasma

amyloid-beta (Abeta) equilibrium in a mouse model of Alzheimer's disease, *Journal of neurochemistry.* **81**, 229-36.

7. Gottfried-Blackmore, A., Sierra, A., Jellinck, P. H., McEwen, B. S. & Bulloch, K. (2008) Brain microglia express steroid-converting enzymes in the mouse, *J Steroid Biochem Mol Biol.* **109**, 96-107.

8. Liu, H. T., Tashmukhamedov, B. A., Inoue, H., Okada, Y. & Sabirov, R. Z. (2006) Roles of two types of anion channels in glutamate release from mouse astrocytes under ischemic or osmotic stress, *Glia.* **54**, 343-57.

9. Heuer, E., Rosen, R. F., Cintron, A. & Walker, L. C. (2012) Nonhuman primate models of Alzheimer-like cerebral proteopathy, *Curr Pharm Des.* **18**, 1159-69.

10. Oikawa, N., Kimura, N. & Yanagisawa, K. (2010) Alzheimer-type tau pathology in advanced aged nonhuman primate brains harboring substantial amyloid deposition, *Brain Res.* **1315**, 137-49.

11. Kimura, N., Yanagisawa, K., Terao, K., Ono, F., Sakakibara, I., Ishii, Y., Kyuwa, S. & Yoshikawa, Y. (2005) Age-related changes of intracellular Abeta in cynomolgus monkey brains, *Neuropathol Appl Neurobiol.* **31**, 170-80.

12. Thery, C. (2011) Exosomes: secreted vesicles and intercellular communications, *F1000 Biol Rep.* **3**, 15.

13. Kimura, N., Inoue, M., Okabayashi, S., Ono, F. & Negishi, T. (2009) Dynein dysfunction induces endocytic pathology accompanied by an increase in Rab GTPases: a potential mechanism underlying age-dependent endocytic dysfunction, *J Biol Chem.* **284**, 31291-302.

14. Kimura, N., Okabayashi, S. & Ono, F. (2014) Dynein dysfunction disrupts beta-amyloid clearance in astrocytes through endocytic disturbances, *Neuroreport.* **25**, 514-20.

15. Cataldo, A. M., Barnett, J. L., Pieroni, C. & Nixon, R. A. (1997) Increased neuronal endocytosis and protease delivery to early endosomes in sporadic Alzheimer's disease: neuropathologic evidence for a mechanism of increased beta-amyloidogenesis, *J Neurosci.* **17**, 6142-51.

16. Cataldo, A. M., Petanceska, S., Terio, N. B., Peterhoff, C. M., Durham, R., Mercken, M., Mehta, P. D., Buxbaum, J., Haroutunian, V. & Nixon, R. A. (2004) Abeta localization in abnormal endosomes: association with earliest Abeta elevations in AD and Down syndrome, *Neurobiol Aging.* **25**, 1263-72.

17. Saman, S., Kim, W., Raya, M., Visnick, Y., Miro, S., Jackson, B., McKee, A. C., Alvarez, V. E., Lee, N. C. & Hall, G. F. (2012) Exosome-associated tau is secreted in tauopathy models and is selectively phosphorylated in cerebrospinal fluid in early Alzheimer disease, *J Biol Chem.* **287**, 3842-9.

Figure legends

Fig.1 Exosomes associate with Aß in the CSF of cynomolgus monkeys. (A) Aß levels in the brain tissues were analyzed. Values are presented as the mean ± SD (Young, n=5; Adult, n=6; Aged, n=9, *p<0.05, ***p<0.001). (B) Images of the exosome fraction. Bars: 1 µm in left panel, 100 nm in right panel. (C) Particle size distribution of the exosome fraction. (D) Western blotting of the exosomes. Alix, flotillin-1(Flot-1), and ganglioside GM1 (GM1) as exosome markers; transferrin receptor (TfR) and GM130 as negative markers. BT, brain tissues (E) Aß levels in the CSF-exosomes were measured. Values are presented as the mean ± SD (Young, n=9; Adult, n=8; Aged, n=4, *p<0.05).

Fig.2 Age-dependent alterations in the concentrations of exosomes from APP mouse CSF. (A) Aß in whole brain tissues (5 µg protein) and in exosomes isolated from the CSF (50 µl) of 13-month-old APP mice was detected. (B) Exosomes derived from 13-month-old APP mouse CSF were negatively stained and immunolabeled for Aß. Scale bar, 50 nm. (C) CSF was collected from APP mice at the indicated ages, and the densities of the exosomes were measured. Aß levels in whole brains of APP mice were quantified. Values of Aß levels are presented as the mean ± SD (n=5).

Fig.3 GSL-enriched neuronal exosomes associate with Aß. Exosomes were collected from primary cultures of cortical neurons (DIV7), astrocytes, and microglia. (A) Total amounts of GSL-glycans and the number of sialic acid moieties in the exosomes were measured. (B) Representative images of fluorescent Aß binding on exosomes after a 5 h exposure. Bar, 100 µm. (C) After a 5 h incubation, ThT fluorescence intensities were detected in solutions containing Aß and exosomes, untreated or pretreated with EGCase. Each column represents the average ± SD of four values.

Fig. 4. Neuronal exosomes decreases Aß pathology in APP mouse brains. Neuronal exosomes were infused into the hippocampus of 13-month-old APP mice for 14 days.

(A) Image of Aß-stained hippocampal section. Bar, 200 μm. (B-C) Aβ-immunopositive areas (B) and the numbers of ThS-positive plaques (C) in each hippocampal region were measured (n = 4 animals, 2 sections per brain; **p<0.01). (D) Hippocampal Aßs were analyzed by ELISA. (n= 5 animals; **p<0.01, ***p<0.001).

Supplemental Information

Materials and Methods

Thin-layer chromatography

Total lipids of the exosomes (1 mg protein) were extracted in chloroform/methanol/water (10 : 5 : 3 by volume). The upper phase was removed and the solvent was evaporated and solubilized in chloroform/methanol (2 : 1 by volume). Total volume of lipid extract was spotted onto high performance thin-layer chromatography plates (Merck, Darmstadt, Germany) and separated with a solvent (chloroform/methanol/0.2% $CaCl_2$, 55 : 45 : 10). After the separation, the plates were thoroughly dried and coated with 0.1% polyisobutylmethacrylate/n-hexane for 1 min. The plate was overlaid with 1% bovine serum albumin/PBS buffer for 20 min at room temperature and then with primary antibodies at 4 °C overnight. After washing with PBS buffer containing 0.05% Tween 20, GM1, GM3, and GD1b were then visualized with horseradish-peroxidase-conjugated cholera toxin B subunit (CTB, Sigma-Aldrich, St. Louis, Missouri, USA), and antibodies specific to GM3 (Nippon Bio-Test Laboratories Inc., Tokyo, Japan), or GD1b (kindly provide by Dr. Robert K. Yu, Department of Neuroscience and Regenerative Medicine, Medical College of Georgia, Georgia Regents University), respectively.

Figure Legends

Supplemental Fig. 1. Aß levels in exosome-free CSF of cynomolgus monkeys. The exosomes were isolated from the monkey CSF, and the rest of CSF (exosome-free) was measured by ELISA for Aß. Values are presented as the mean ± SD (Young, n=9; Adult, n=8; Aged, n=4. ***$p<0.001$).

Supplemental Fig. 2. The particle numbers and GSL-profiles of the exosomes derived from primary cultured neurons. Exosomes were collected from culture medium of cortical neurons (DIV1, 7, or 14). (A) The particle number of the exosomes derived from 1 x 10^7 cells were measured using qNano system. (Values are the mean±SD, n=3, *$p<0.05$, **$p<0.01$) (B) The amount of GSL-glycans in the exosomes were analyzed by mass spectrometry. GSLs were classified according to the number of sialic acid moieties. Data was determined by standardization with protein content and expressed as

percentage of DIV1.

Supplemental Fig. 3. Immunoblot analysis of GM3, GM1, or GD1b in the neuronal and glial exosomes. Exosomes were collected from primary cultures of cortical neurons (DIV7), astrocytes, and microglia. Total lipids, which were extracted from the exosomes, and standard GSLs (std., 0.1 μg) were separated by thin-layer chromatography and visualized with CTB or antibodies specific to GM3 or GD1b, respectively.

Figure 1

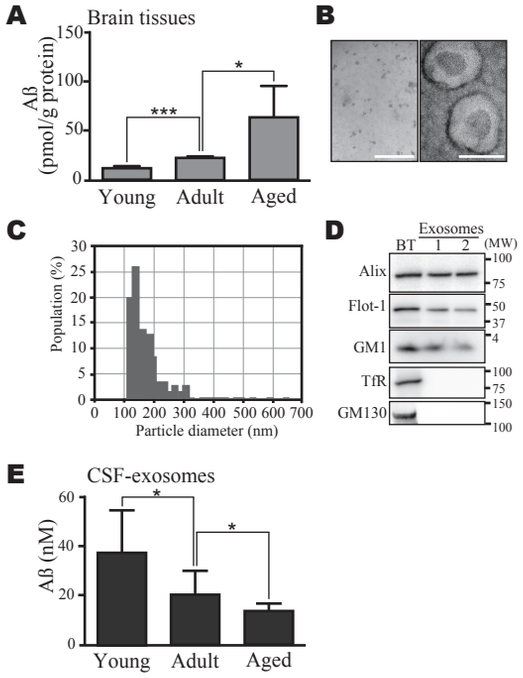
A
Brain tissues
Aß (pmol/g protein)
150
100
50
0
***
*
Young
Adult
Aged
B
C
Population (%)
30
25
20
15
10
5
0
0 100 200 300 400 500 600 700
Particle diameter (nm)
D
Exosomes
BT 1 2
(MW)
Alix
Flot-1
GM1
TfR
GM130
100
75
50
37
4
100
75
150
100
E
CSF-exosomes
Aß (nM)
60
40
20
0
*
*
Young
Adult
Aged

Figure 2

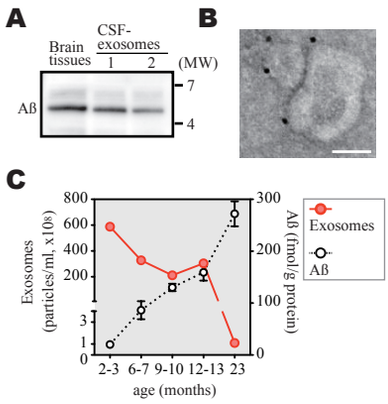
A
Brain tissues
CSF-exosomes
1
2
(MW)
Aß
7
4
B
C
Exosomes (particles/ml, x10⁸)
800
600
400
200
3
1
0
Aß (fmol/g protein)
300
200
100
0
2-3
6-7
9-10
12-13
23
age (months)
Exosomes
Aß

Figure 3

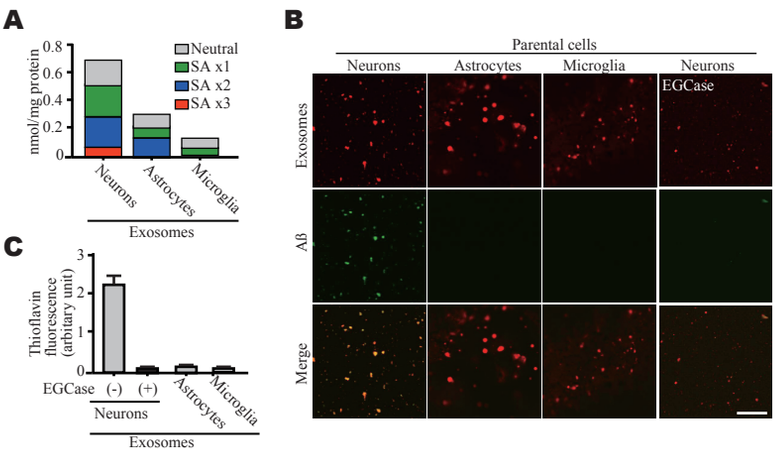
A
nmol/mg protein
0.8
0.6
0.4
0.2
0
Neutral
SA x1
SA x2
SA x3
Neurons
Astrocytes
Microglia
Exosomes
B
Parental cells
Neurons
Astrocytes
Microglia
Neurons
EGCase
Exosomes
Aß
Merge
C
Thioflavin fluorescence (arbitary unit)
3
2
1
0
EGCase (-) (+)
Neurons
Astrocytes
Microglia
Exosomes

Figure 4

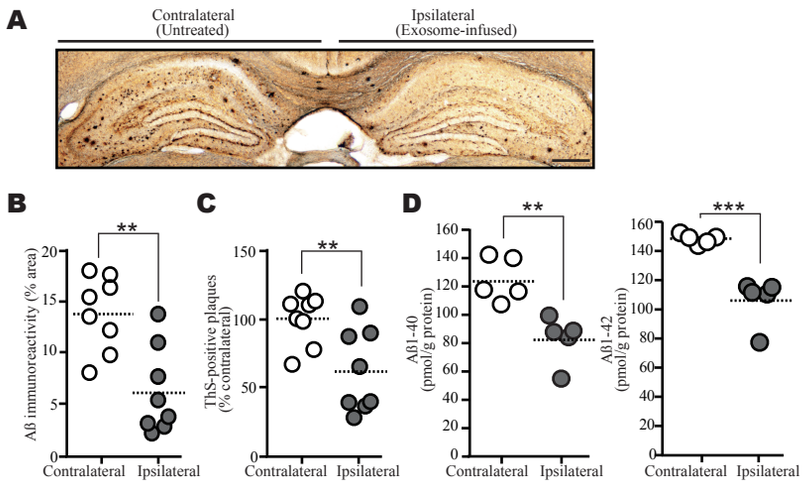
A
Contralateral
(Untreated)
Ipsilateral
(Exosome-infused)
B
Aß immunoreactivity (% area)
**
Contralateral
Ipsilateral
C
ThS-positive plaques
(% contralateral)
**
Contralateral
Ipsilateral
D
Aß1-40
(pmol/g protein)
**
Contralateral
Ipsilateral
Aß1-42
(pmol/g protein)
***
Contralateral
Ipsilateral

Supplemental figure 1

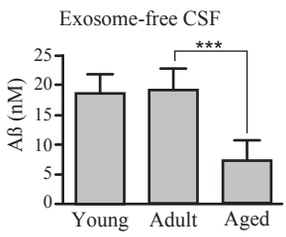

Supplemantal figure 2

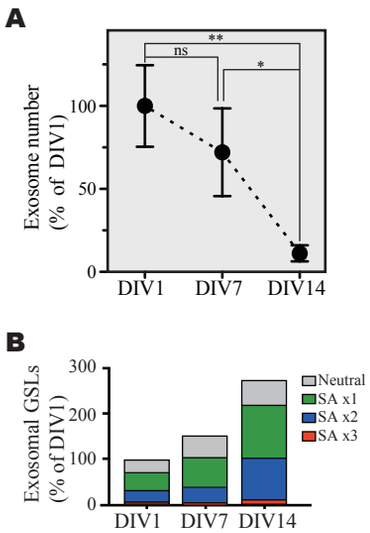

Supplemental figure 3

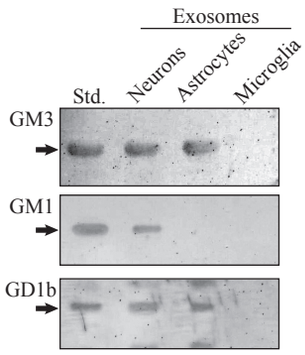

Supplemental Table

Summary of exosomal profiles of GSL-glycans in rodent primary cultures of cortical neurons, astrocytes, and microglia

Absolute quantity (pmol/mg protein)

No.	Compsition	Class	Name	Neurons	Astrocytes	Microglia
1	(Hex)2	Lac	LacCer	16.66	18.68	6.52
2	(Hex)2(Neu5Ac)1	Gg	GM3	30.72	51.82	4.72
3	(Hex)2(HexNAc)1(Neu5Ac)1	Gg	GM2	18.22	2.10	0.00
4	(Hex)2(Neu5Ac)2	Gg	GD3	2.44	0.00	0.00
5	(Hex)3(HexNAc)1(Neu5Ac)1	Gg	GM1	131.41	20.23	4.25
6	(Hex)3(HexNAc)1(Fuc)1(Neu5Ac)1	Gg	Fuc-GM1	2.31	2.38	2.60
7	(Hex)3(HexNAc)1(Neu5Ac)2	Gg	GD1	197.60	115.18	4.21
8	(Hex)3(HexNAc)1(Neu5Ac)1(Neu5Gc)1	Gg	GD1(Gc)	3.41	4.24	2.03
9	(Hex)3(HexNAc)1(Neu5Gc)2	Gg	GD1(Gc2)	1.02	1.04	0.00
10	(Hex)3(HexNAc)2(NeuAc)2	Gg	GalNAc-GD1	0.00	0.00	0.00
11	(Hex)3(HexNAc)2(NeuAc)3 lactone	Gg	GT1 (lactone)	96.32	0.00	0.00
12	(Hex)3	Gb	Gb3	26.69	46.13	20.08
13	(Hex)3(HexNAc)1	Gb	Gb4	45.20	23.92	11.93
14	(Hex)4(HexNAc)1(Fuc)1	Gb	globoH	9.59	0.00	0.00
15	(Hex)4(HexNAc)1(Neu5Ac)1	Gb	SSEA-4	4.19	6.87	5.27
16	(Hex)3(HexNAc)1(Fuc)1	(n)Lc	Fuc-(n)Lc4 (SSEA-1)	9.22	0.00	0.00
17	(Hex)4(HexNAc)1	(n)Lc	Gal-(n)Lc4	6.11	7.96	23.09
19	(Hex)3(HexNAc)2	(n)Lc	(n)Lc5	46.42	2.80	0.00
20	(Hex)3(HexNAc)2(Fuc)1	(n)Lc	Fuc-(n)Lc5 (type I A)	0.00	0.00	0.00
21	(Hex)4(HexNAc)2	(n)Lc	nLc6	2.53	2.11	0.00
22	(Hex)3(HexNAc)2(Neu5Ac)1	(n)Lc		1.79	0.00	0.00
23	(Hex)4(HexNAc)2(Fuc)1	(n)Lc	(Type II H etc)	6.89	0.00	0.00
24	(Hex)5(HexNAc)2	(n)Lc		1.38	1.58	2.49
25	(Hex)4(HexNAc)3	(n)Lc		0.00	0.00	0.00
26	(Hex)4(HexNAc)2(Fuc)2	(n)Lc	(Ley, dimeric Lex)	7.48	0.00	0.00
27	(Hex)4(HexNAc)2(Neu5Ac)1	(n)Lc		23.37	2.98	2.34
28	(Hex)4(HexNAc)2(Fuc)1(Neu5Ac)1	(n)Lc		3.13	0.00	0.00
29	(Hex)4(HexNAc)3(Neu5Ac)1	(n)Lc		0.00	0.00	0.00
30	(Hex)5(HexNAc)4	(n)Lc		1.49	0.00	0.00
31	(Hex)5(HexNAc)3(Fuc)2	(n)Lc		1.06	0.00	0.00
32	(Hex)5(HexNAc)3(Neu5Ac)1	(n)Lc		0.65	0.04	1.73
33	(Hex)5(HexNAc)3(Fuc)1(Neu5Ac)1	(n)Lc		4.58	0.00	0.00
34	(Hex)2(HexNAc)1	-	Lc3/aGM2	0.00	0.29	8.18
35	(Hex)2(HexNAc)2	-		1.52	0.00	0.00
36	(Hex)5(HexNAc)1	-		0.00	0.00	0.00
37	(Hex)3(HexNAc)3	-		0.00	0.00	0.00
			total	703.40	310.35	99.42

Relative quantity (%)

No.	Compsition	Class	Name	Neurons	Astrocytes	Microglia
1	(Hex)2	Lac	LacCer	2.37	6.02	6.56
2	(Hex)2(Neu5Ac)1	Gg	GM3	4.37	16.70	4.75
3	(Hex)2(HexNAc)1(Neu5Ac)1	Gg	GM2	2.59	0.68	0.00
4	(Hex)2(Neu5Ac)2	Gg	GD3	0.35	0.00	0.00
5	(Hex)3(HexNAc)1(Neu5Ac)1	Gg	GM1	18.68	6.52	4.28
6	(Hex)3(HexNAc)1(Fuc)1(Neu5Ac)1	Gg	Fuc-GM1	0.33	0.77	2.61
7	(Hex)3(HexNAc)1(Neu5Ac)2	Gg	GD1	28.09	37.11	4.24
8	(Hex)3(HexNAc)1(Neu5Ac)1(Neu5Gc)1	Gg	GD1(Gc)	0.48	1.37	2.04
9	(Hex)3(HexNAc)1(Neu5Gc)2	Gg	GD1(Gc2)	0.14	0.33	0.00
10	(Hex)3(HexNAc)2(NeuAc)2	Gg	GalNac-GD1	0.00	0.00	0.00
11	(Hex)3(HexNAc)2(NeuAc)3 lactone	Gg	GT1 (lactone)	13.69	0.00	0.00
12	(Hex)3	Gb	Gb3	3.79	14.86	20.19
13	(Hex)3(HexNAc)1	Gb	Gb4	6.43	7.71	12.00
14	(Hex)4(HexNAc)1(Fuc)1	Gb	globoH	1.36	0.00	0.00
15	(Hex)4(HexNAc)1(Neu5Ac)1	Gb	SSEA-4	0.60	2.21	5.30
16	(Hex)3(HexNAc)1(Fuc)1	(n)Lc	Fuc-(n)Lc4 (SSEA-1)	1.31	0.00	0.00
17	(Hex)4(HexNAc)1	(n)Lc	Gal-(n)Lc4	0.87	2.57	23.23
19	(Hex)3(HexNAc)2	(n)Lc	(n)Lc5	6.60	0.90	0.00
20	(Hex)3(HexNAc)2(Fuc)1	(n)Lc	Fuc-(n)Lc5 (type I A)	0.00	0.00	0.00
21	(Hex)4(HexNAc)2	(n)Lc	nLc6	0.36	0.68	0.00
22	(Hex)3(HexNAc)2(Neu5Ac)1	(n)Lc		0.25	0.00	0.00
23	(Hex)4(HexNAc)2(Fuc)1	(n)Lc	(Type II H etc)	0.98	0.00	0.00
24	(Hex)5(HexNAc)2	(n)Lc		0.20	0.51	2.50
25	(Hex)4(HexNAc)3	(n)Lc		0.00	0.00	0.00
26	(Hex)4(HexNAc)2(Fuc)2	(n)Lc	(Ley, dimeric Lex)	1.06	0.00	0.00
27	(Hex)4(HexNAc)2(Neu5Ac)1	(n)Lc		3.32	0.96	2.35
28	(Hex)4(HexNAc)2(Fuc)1(Neu5Ac)1	(n)Lc		0.45	0.00	0.00
29	(Hex)4(HexNAc)3(Neu5Ac)1	(n)Lc		0.00	0.00	0.00
30	(Hex)5(HexNAc)4	(n)Lc		0.21	0.00	0.00
31	(Hex)5(HexNAc)3(Fuc)2	(n)Lc		0.15	0.00	0.00
32	(Hex)5(HexNAc)3(Neu5Ac)1	(n)Lc		0.09	0.01	1.74
33	(Hex)5(HexNAc)3(Fuc)1(Neu5Ac)1	(n)Lc		0.65	0.00	0.00
34	(Hex)2(HexNAc)1	-	Lc3/aGM2	0.00	0.09	8.23
35	(Hex)2(HexNAc)2	-		0.22	0.00	0.00
36	(Hex)5(HexNAc)1	-		0.00	0.00	0.00
37	(Hex)3(HexNAc)3	-		0.00	0.00	0.00
			total	100.00	100.00	100.00